




# Insights into Nitrate-Reducing Fe(II) Oxidation Mechanisms through Analysis of Cell-Mineral Associations, Cell Encrustation, and Mineralogy in the Chemolithoautotrophic Enrichment Culture KS

M. Nordhoff,<sup>a</sup> C. Tominski,<sup>a</sup> M. Halama,<sup>a</sup> J. M. Byrne,<sup>a</sup> M. Obst,<sup>b</sup>  S. Kleindienst,<sup>a</sup> S. Behrens,<sup>a,c</sup> A. Kappler<sup>a,d</sup>

Geomicrobiology, Center for Applied Geosciences, University of Tuebingen, Tuebingen, Germany<sup>a</sup>; Bayreuth Center for Ecology and Environmental Research, University of Bayreuth, Bayreuth, Germany<sup>b</sup>; Department of Civil, Environmental, and Geo-Engineering, University of Minnesota, Minneapolis, Minnesota, USA<sup>c</sup>; Center for Geomicrobiology, Department of Bioscience, Aarhus University, Aarhus, Denmark<sup>d</sup>

**ABSTRACT** Most described nitrate-reducing Fe(II)-oxidizing bacteria (NRFeOB) are mixotrophic and depend on organic cosubstrates for growth. Encrustation of cells in Fe(III) minerals has been observed for mixotrophic NRFeOB but not for autotrophic phototrophic and microaerophilic Fe(II) oxidizers. So far, little is known about cell-mineral associations in the few existing autotrophic NRFeOB. Here, we investigate whether the designated autotrophic Fe(II)-oxidizing strain (closely related to *Gallionella* and *Sideroxydans*) or the heterotrophic nitrate reducers that are present in the autotrophic nitrate-reducing Fe(II)-oxidizing enrichment culture KS form mineral crusts during Fe(II) oxidation under autotrophic and mixotrophic conditions. In the mixed culture, we found no significant encrustation of any of the cells both during autotrophic oxidation of 8 to 10 mM Fe(II) coupled to nitrate reduction and during cultivation under mixotrophic conditions with 8 to 10 mM Fe(II), 5 mM acetate, and 4 mM nitrate, where higher numbers of heterotrophic nitrate reducers were present. Two pure cultures of heterotrophic nitrate reducers (*Nocardioides* and *Rhodanobacter*) isolated from culture KS were analyzed under mixotrophic growth conditions. We found green rust formation, no cell encrustation, and only a few mineral particles on some cell surfaces with 5 mM Fe(II) and some encrustation with 10 mM Fe(II). Our findings suggest that enzymatic, autotrophic Fe(II) oxidation coupled to nitrate reduction forms poorly crystalline Fe(III) oxyhydroxides and proceeds without cellular encrustation while indirect Fe(II) oxidation via heterotrophic nitrate-reduction-derived nitrite can lead to green rust as an intermediate mineral and significant cell encrustation. The extent of encrustation caused by indirect Fe(II) oxidation by reactive nitrogen species depends on Fe(II) concentrations and is probably negligible under environmental conditions in most habitats.

**IMPORTANCE** Most described nitrate-reducing Fe(II)-oxidizing bacteria (NRFeOB) are mixotrophic (their growth depends on organic cosubstrates) and can become encrusted in Fe(III) minerals. Encrustation is expected to be harmful and poses a threat to cells if it also occurs under environmentally relevant conditions. Nitrite produced during heterotrophic denitrification reacts with Fe(II) abiotically and is probably the reason for encrustation in mixotrophic NRFeOB. Little is known about cell-mineral associations in autotrophic NRFeOB such as the enrichment culture KS. Here, we show that no encrustation occurs in culture KS under autotrophic and mixotrophic conditions while heterotrophic nitrate-reducing isolates from culture KS become en-

Received 30 March 2017 Accepted 25 April 2017

Accepted manuscript posted online 28 April 2017

**Citation** Nordhoff M, Tominski C, Halama M, Byrne JM, Obst M, Kleindienst S, Behrens S, Kappler A. 2017. Insights into nitrate-reducing Fe(II) oxidation mechanisms through analysis of cell-mineral associations, cell encrustation, and mineralogy in the chemolithoautotrophic enrichment culture KS. *Appl Environ Microbiol* 83:e00752-17. <https://doi.org/10.1128/AEM.00752-17>.

**Editor** Joel E. Kostka, Georgia Institute of Technology

**Copyright** © 2017 American Society for Microbiology. All Rights Reserved.

Address correspondence to A. Kappler, [andreas.kappler@uni-tuebingen.de](mailto:andreas.kappler@uni-tuebingen.de).

crusted. These findings support the hypothesis that encrustation in mixotrophic cultures is caused by the abiotic reaction of Fe(II) with nitrite and provide evidence that Fe(II) oxidation in culture KS is enzymatic. Furthermore, we show that the extent of encrustation caused by indirect Fe(II) oxidation by reactive nitrogen species depends on Fe(II) concentrations and is probably negligible in most environmental habitats.

**KEYWORDS** nitrate-dependent Fe(II) oxidation, cell-mineral aggregates, green rust

Nitrate-reducing Fe(II)-oxidizing bacteria (NRFeOB) have been found in soils, freshwater, brackish water, and marine environments (1–9). They link the nitrogen, carbon, and Fe cycles and potentially play a major role in Fe cycling. The products of microbial Fe(II) oxidation coupled to nitrate reduction are Fe(III) minerals and dinitrogen or intermediates of the denitrification pathway, e.g.,  $\text{NO}_2^-$ , NO, and  $\text{N}_2\text{O}$  (10–12). Most described NRFeOB require an organic cosubstrate to allow for their continuous cultivation and continuous oxidation of Fe(II) to Fe(III) (1, 2, 6, 9–11, 13–20). Therefore, they are frequently referred to as mixotrophic NRFeOB.

Despite the relatively large number of described mixotrophic NRFeOB, examples of autotrophic NRFeOB are rare. The enrichment culture KS described by Straub et al. (10) was the first described NRFeOB culture capable of autotrophic growth by Fe(II) oxidation coupled to nitrate reduction that can be maintained continuously under chemolithoautotrophic conditions. Since then, only a few pure cultures capable of autotrophic nitrate-reducing Fe(II) oxidation (NRFeO) have been described in the literature (4, 5, 8, 10, 21–28). However, the ability for continuous Fe(II) oxidation and growth under autotrophic conditions over several generations has not yet been shown for all of these cultures. In the environment, the existence of autotrophic NRFeOB in marine sediments has been demonstrated recently (29).

The autotrophic culture KS is dominated by a strain belonging to the family of *Gallionellaceae* (closely related to *Sideroxydans lithotrophicus* ES-1 and *Gallionella capsiferiformans* ES-2). This strain, here referred to as *Gallionellaceae* sp., was designated the autotrophic Fe(II) oxidizer in the culture (30). In the culture used in this study, it accounts for 96% of the total community under autotrophic growth conditions with Fe(II) and nitrate (31). In another version of culture KS from a different laboratory, which also has different community members, *Gallionellaceae* sp. accounts for only 42% of the total community under autotrophic conditions (31). It has to be taken into account, however, that this culture has been transferred with a 10% inoculum for years while ours was transferred with a 1% inoculum, also for years (31). Previous studies found evidence that the remainder of the community in culture KS consists of strains that are not capable of autotrophic NRFeO but are heterotrophic nitrate reducers (10, 30). However, a recent metagenomic study also found genes for  $\text{CO}_2$  fixation in the genome of these strains (31). In our autotrophically grown culture, these additional strains are *Rhodanobacter* sp. (1%), *Bradyrhizobium* sp. (1%), *Nocardioides* sp. (<1%), *Polaromonas* sp. (<1%), and *Thiobacillus* sp. (<1%) (31). Culture KS can also be cultivated under mixotrophic growth conditions with Fe(II), nitrate, and acetate. In this case, the relative abundance of the *Bradyrhizobium* sp. increases to a maximum of 83% while the relative abundance of *Gallionellaceae* sp. decreases to ca. 4 to 13% (although the absolute cell numbers of the *Gallionellaceae* sp. remain the same under mixotrophic as under autotrophic growth conditions while the cell numbers of the other heterotrophic strains increase under mixotrophic conditions [C. Tominski, A. Kappler, and S. Behrens, unpublished data]).

Under autotrophic conditions, culture KS can oxidize free, dissolved Fe(II), i.e.,  $\text{Fe}^{2+}$ , almost completely [ $>90\%$  of 10 mM Fe(II)] and reduces nitrate to  $\text{N}_2$  (31). In addition, it can oxidize poorly soluble Fe(II)-bearing minerals (10, 32, 33). So far, all attempts to obtain a pure culture of the Fe(II)-oxidizing *Gallionellaceae* sp. strain have failed. Despite the sequence similarity to *Gallionella lithotrophicus* ES-1 and *Gallionella capsiferiformans* ES-2, microaerophilic Fe(II) oxidation by culture KS could not be demonstrated so

far (30). Although potential mutual dependencies between the different bacterial strains in culture KS are not fully understood, recent metagenomics analyses suggest a dependence of *Gallionellaceae* sp. on the other bacteria for complete denitrification to  $N_2$  (31).

Similarly to other Fe(II)-oxidizing cultures growing at neutral pH, culture KS faces the problem that the Fe(III) produced by microbial Fe(II) oxidation is poorly soluble at neutral pH. Therefore, neutrophilic Fe(II)-oxidizing bacteria are thought to need a means to dispose their metabolic product to avoid cell encrustation in Fe minerals, which is expected to be harmful to cells (34). We are interested in determining whether cells get encrusted or not, in particular because it has been suggested that encrustation could hinder metabolism, e.g., the uptake of substrates and/or nutrients and the efflux of metabolites, possibly leading to cell death (35). Furthermore, metabolic inactivity as a result of encrustation has been reported (3). While autotrophic phototrophic and autotrophic microaerophilic Fe(II)-oxidizing bacteria can prevent encrustation (36–38), tight surface coverage of mixotrophic NRFeOB cells is frequently observed in batch cultures (3, 9, 35, 39). Klueglein et al. (35) observed encrustation of the NRFeOB *Acidovorax* sp. strain BoFeN1 and *Pseudogulbenkiania* sp. strain 2002 cultivated with Fe(II), nitrate, and acetate. Fe(II) oxidation and encrustation also occurred in cultures of the two ordinary heterotrophic denitrifying bacterial strains *Paracoccus denitrificans* ATCC 19367 and *P. denitrificans* Pd 1222 under the same growth conditions. Accumulation of up to 1 mM nitrite in all of these cultures is thought to be responsible for abiotic Fe(II) oxidation that causes cell encrustation. These findings raise the questions of (i) to what extent Fe(II) oxidation is observed in cultures of mixotrophic NRFeOB due to enzymatic Fe(II) oxidation, (ii) to what extent it is caused by abiotic Fe(II) oxidation by reactive nitrogen species, and (iii) whether autotrophic NRFeOB also become encrusted in Fe(III) minerals. In order to answer these questions, in particular the third question, the goal of the present study was to determine if any cell encrustation occurs in the culture KS during autotrophic nitrate-reducing Fe(II) oxidation. The second goal of the study was to find out whether under mixotrophic growth conditions [with Fe(II), acetate, and nitrate] any of the heterotrophic nitrate reducers in the culture KS become encrusted in Fe(III) minerals, e.g., as a consequence of abiotic Fe(II) oxidation by reactive nitrogen species.

## RESULTS

**Fe(II) oxidation, nitrate reduction, and acetate consumption.** Culture KS was cultivated under autotrophic and mixotrophic growth conditions. Under autotrophic conditions (Fig. 1A), culture KS oxidized Fe(II) almost completely (7.1 mM of 8.2 mM, i.e., 87%) and reduced 1.6 mM of 3.4 mM nitrate (47%) within 4 days. The majority of the Fe(II) oxidation and nitrate reduction occurred during the exponential growth phase within the 3rd day of incubation, and only small amounts of Fe(II) were oxidized afterward. Under mixotrophic growth conditions (Fig. 1B), 7.2 mM of 9.9 mM Fe(II) (73%) was oxidized within 7 days. At the same time, 2.8 mM nitrate (100%) and 1.7 mM of 4.5 mM acetate (38%) were consumed. In contrast to autotrophic growth conditions, under mixotrophic conditions significant Fe(II) and nitrate consumption started later (3 days after inoculation) and proceeded over a longer period of time. The majority of Fe(II) and nitrate was consumed between 3 and 7 days after inoculation. Cell counts in combination with fluorescence *in situ* hybridization analysis (data not shown) revealed that under autotrophic growth conditions the total cell numbers increased from  $1 \times 10^5$  cells/ml to  $2 \times 10^7$  cells/ml with up to 97.5% of the cells represented by the designated Fe(II)-oxidizing *Gallionellaceae* sp. at the end of Fe(II) oxidation. In contrast, under mixotrophic conditions total cell numbers increased from  $1 \times 10^5$  cells/ml to  $1 \times 10^8$  cells/ml with only 10% of the cells represented by *Gallionellaceae* sp. while the remaining 90% were cells from the heterotrophic community (*Bradyrhizobium* [83%], *Rhodanobacter*, and *Nocardioiodes*).

In addition to the mixed culture KS that contained several strains, a *Nocardioiodes* strain and a *Rhodanobacter* strain, which were both isolated from culture KS, were

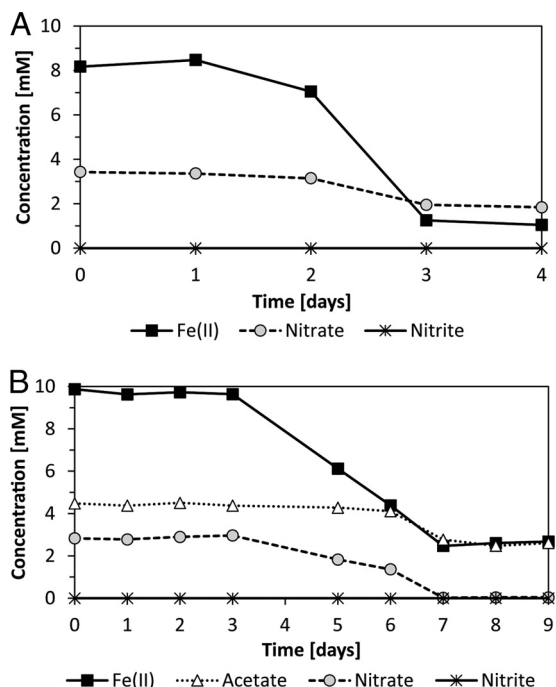


**FIG 1** Concentrations of Fe(II), nitrate, and nitrite in culture KS cultivated under autotrophic (A) and mixotrophic (B) growth conditions. Acetate consumption is shown for mixotrophic conditions (B).

cultivated individually. These two strains did not grow individually under autotrophic conditions with Fe(II) and nitrate (Tominski et al., unpublished), but they grew and showed Fe(II) oxidation under mixotrophic growth conditions. Both isolates were cultivated in mixotrophic setups either with 10 mM Fe(II) or with 5 mM Fe(II) (Table 1). In addition, these setups contained 5 mM acetate and 4 mM nitrate. We found that after 14 days the *Nocardioides* sp. culture oxidized 1.8 mM of 5.6 mM (32%) and 4.4 mM of 9.3 mM (47%) Fe(II) and the *Rhodanobacter* sp. culture oxidized 1.5 mM of 5.3 mM (28%) and 4.3 mM of 9.6 mM (45%) Fe(II). The *Nocardioides* strain accumulated up to 2.1 mM nitrite in the presence of 5 mM Fe(II) and up to 0.6 mM nitrite in the presence of 10 mM

**TABLE 1** Nitrate and acetate consumption, oxidation of Fe(II), and nitrite accumulation by *Nocardioides* sp. and *Rhodanobacter* sp. isolated from enrichment culture KS

Initial mixture, species, and day of expt	Concn (mM)			
	Nitrate	Acetate	Fe(II)	Nitrite
5 mM Fe(II), 5 mM acetate, 4 mM nitrate				
<i>Rhodanobacter</i> sp.				
Day 0	4.1	4.8	5.3	0
Day 7	1.2	2.4	4.4	0.6
Day 14	0	2.0	3.8	0
<i>Nocardioides</i> sp.				
Day 0	4.1	5.1	5.6	0
Day 7	1.0	4.5	4.6	0.2
Day 14	0.3	3.7	3.8	2.1
10 mM Fe(II), 5 mM acetate, 4 mM nitrate				
<i>Rhodanobacter</i> sp.				
Day 0	3.9	5.6	9.6	0
Day 7	2.3	4.8	8.3	0
Day 14	0.3	2.8	5.3	1.0
<i>Nocardioides</i> sp.				
Day 0	4.3	5.8	9.3	0
Day 7	2.9	5.3	7.9	0.6
Day 14	0.5	3.9	4.9	0.7

Fe(II). The *Rhodanobacter* strain accumulated up to 0.6 mM nitrite in the presence of 5 mM Fe(II) and up to 1.0 mM nitrite in the presence of 10 mM Fe(II). Surprisingly, nitrite was still detected at the end of the incubation, although it is expected to react further with Fe(II), maybe because of a limited protonation of the  $\text{NO}_2^-$ , which then forms  $\text{HNO}_2$ , which decays to the relevant Fe(II) oxidants NO and  $\text{NO}_2$  (40). *Bradyrhizobium* sp. was also isolated from culture KS but did not grow under mixotrophic or autotrophic conditions.

**Cell-mineral associations.** We used confocal laser scanning microscopy (CLSM) in combination with different extracellular polymeric substance (EPS)- and DNA-staining fluorescent dyes to determine the associations of cells with minerals and to determine the presence of EPSs that have been observed in cultures of other Fe(II)-oxidizing bacteria previously (35, 41). CLSM allows for the investigation of hydrated samples and avoids changes and artifacts introduced by sample preparation (such as drying) for electron microscopy, therefore providing a better preservation of cell-mineral associations. We first analyzed culture KS under autotrophic growth conditions (Fig. 2). The signal of the DNA-binding dye showed that most cells are closely associated with mineral particles which are visualized by their reflection of the laser light. The signal of the lectin conjugate that binds to EPS was colocalized with the reflection signal of the minerals, suggesting that EPS is associated with the mineral particles formed during Fe(II) oxidation. The signal of the lectin conjugate was also colocalized with some cells that were associated with mineral particles. Associations of cells with mineral and EPS were judged based on individual slices (thickness of the optical section, 1.163  $\mu\text{m}$ ) of the three-dimensional (3D) data sets from which the projections shown in Fig. 2 to 4 were created. We considered cells that had a lateral distance of less than 2  $\mu\text{m}$  from EPS or minerals to be associated. Based on slice thickness, the distance in z was 1.163  $\mu\text{m}$  or less. When we analyzed culture KS growing under mixotrophic growth conditions, we observed a higher number of cells associated with mineral particles (Fig. 2) than under autotrophic conditions. The fraction of “planktonic” cells that were not associated with mineral particles (Fig. 5) was also higher under mixotrophic conditions. Many of these mineral-associated cells had a different morphology than those observed under autotrophic growth conditions. The association of EPS with minerals appeared to be similar to that observed under autotrophic growth conditions.

Finally, we analyzed the individual *Nocardioides* sp. and *Rhodanobacter* sp. isolated from culture KS by microscopy under mixotrophic growth conditions. Fluorescence microscopy images (Fig. 5) present an overview of all cells, both free and mineral associated, while CLSM images show the association of cells, minerals, and EPS in detail (Fig. 3 and 4). We first cultivated these two strains individually under the same mixotrophic growth conditions as culture KS [10 mM Fe(II), 5 mM acetate, 4 mM nitrate]. We found that the majority of cells in both the *Nocardioides* sp. and *Rhodanobacter* sp. cultures were free and not associated with mineral particles (Fig. 5). However, the few mineral particles that were present had bacteria and also EPS associated with them (Fig. 3 and 4). We also cultivated these two individual pure cultures mixotrophically with lower Fe(II) concentrations [5 mM Fe(II), 5 mM acetate, 4 mM nitrate] since the high Fe(II) concentrations used for cultivation of culture KS could potentially have had toxic and inhibitory effects that decreased in culture KS (which contained all members of the enrichment) when sufficient Fe(II) was oxidized over time. In the presence of 5 mM Fe(II), we found more cells for each of the individual *Nocardioides* sp. and *Rhodanobacter* sp. strains than in the 10 mM setup (Fig. 5), and similarly to the incubations with 10 mM Fe(II), the few mineral particles present had bacteria and EPS associated with them (Fig. 3 and 4).

**Cell encrustation.** We used scanning electron microscopy (SEM) to determine whether cell surfaces were covered with Fe minerals, i.e., whether the cells were encrusted in Fe(III) minerals. For the enrichment culture KS, we screened ca. 100 cells under autotrophic conditions and ca. 200 cells under mixotrophic conditions (due to the higher cell numbers under mixotrophic conditions). For the isolated *Nocardioides*

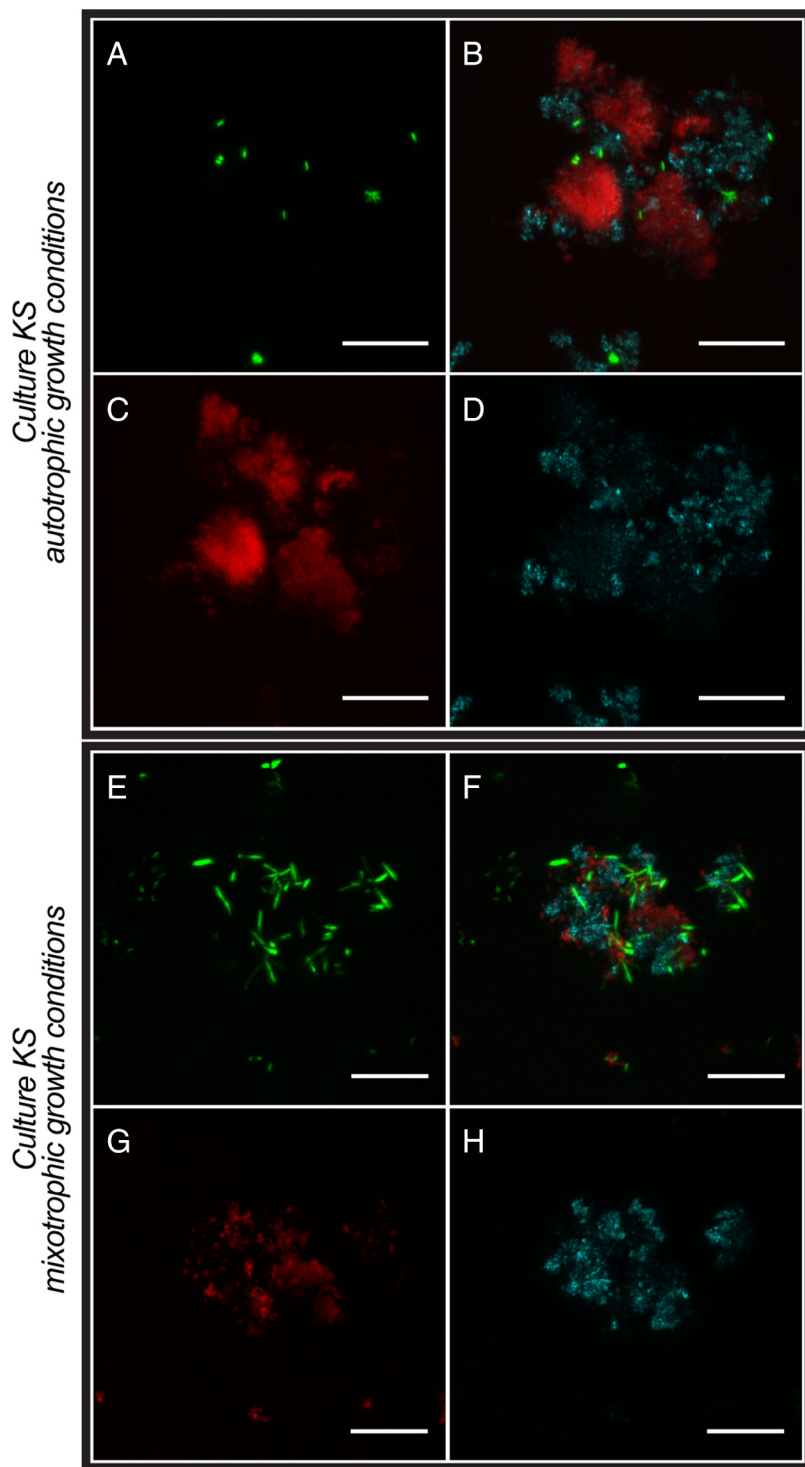


**FIG 2** CLSM images of enrichment culture KS grown under autotrophic conditions (4 days of incubation) (A to D) and mixotrophic conditions (7 days of incubation) (E to H). (A and E) DNA was stained with Syto 9 (green). (C and G) EPS was stained with a peanut agglutinin (PNA)-Alexa Fluor 647 conjugate (red). (D and H) Minerals were visualized by their reflection of the laser (cyan). (B and F) Overlays of the individual channels. Bars, 10  $\mu\text{m}$ .

and *Rhodanobacter* strains, we analyzed ca. 50 cells under mixotrophic conditions for each isolate and for each Fe(II) concentration [5 mM Fe(II) and 10 mM Fe(II)].

The surfaces of individual cells (ca. 1.4  $\mu\text{m}$  long) observed in culture KS cultivated under autotrophic growth conditions were smooth and free of mineral particles

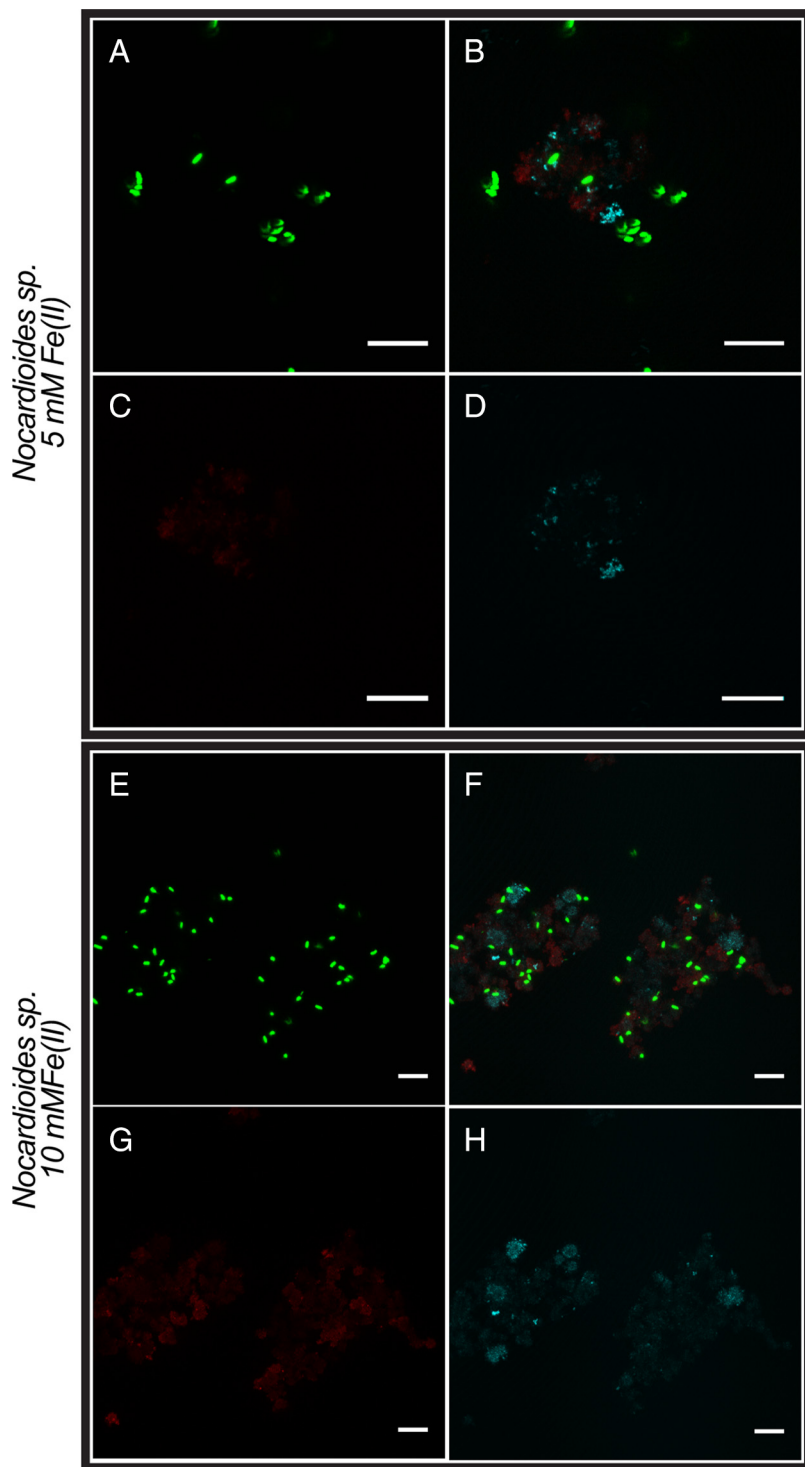


**FIG 3** CLSM images of *Nocardiooides* sp. isolated from enrichment culture KS. Mixotrophic conditions with 5 (A to D) or 10 (E to H) mM Fe(II) (14 days of incubation). (A and E) DNA was stained with Syto 9 (green). (C and G) EPS was stained with a PNA-Alexa Fluor 647 conjugate (red). (D and H) Minerals were visualized by their reflection of the laser (cyan). (B and F) Overlays of the individual channels. Bars, 10  $\mu$ m.

(Fig. 6A, C, and E and 7). A few encrusted cell-shaped structures were found but could not unambiguously be identified as microbial cells. In culture KS cultivated under mixotrophic growth conditions, we found cells with different morphology and size in addition to those observed under autotrophic conditions. This was in accordance with

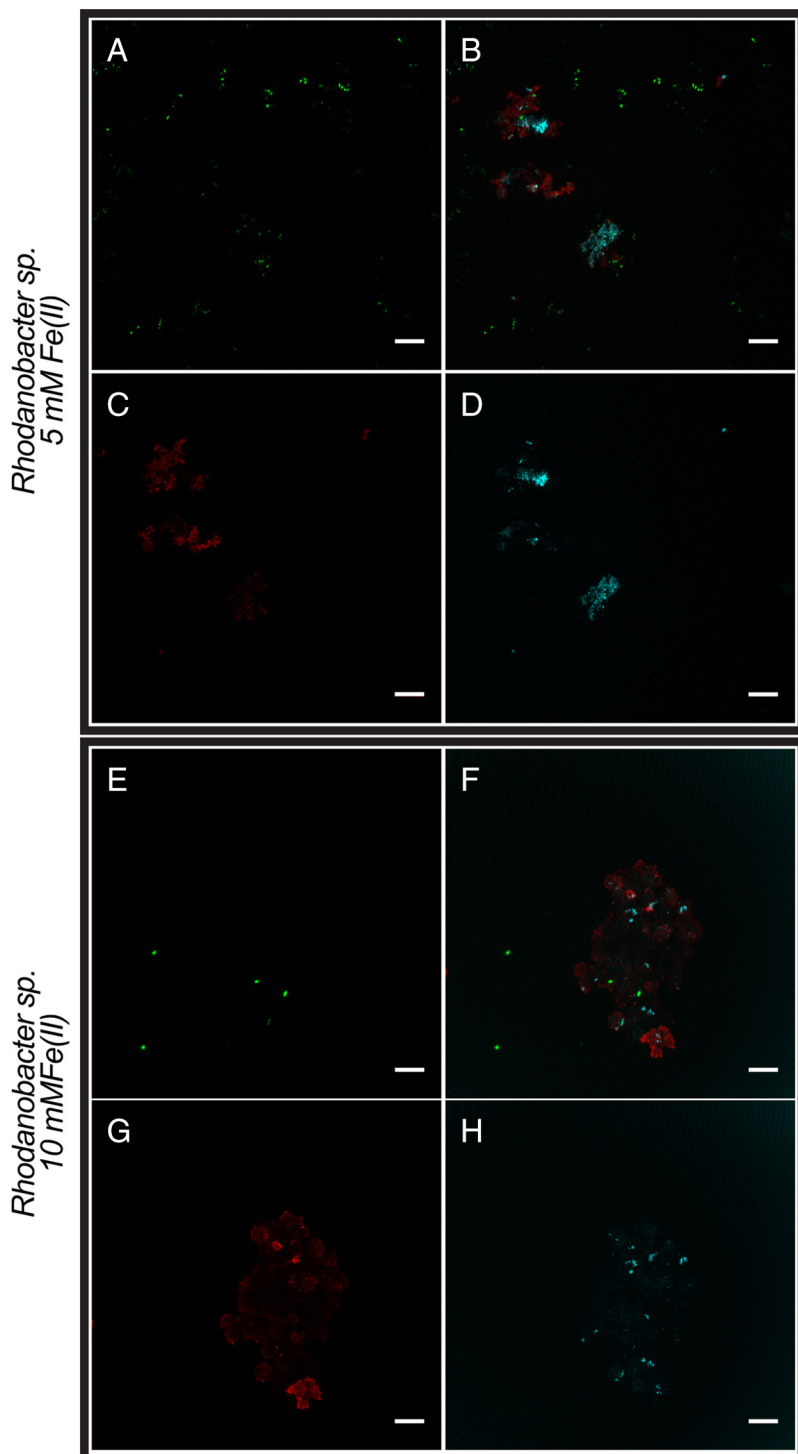


**FIG 4** CLSM images of *Rhodanobacter* sp. isolated from enrichment culture KS. Mixotrophic conditions with 5 (A to D) or 10 (E to H) mM Fe(II) (14 days of incubation). (A and E) DNA was stained with Syto 9 (green). (C and G) EPS was stained with a PNA-Alexa Fluor 647 conjugate (red). (D and H) Minerals were visualized by their reflection of the laser (cyan). (B and F) Overlays of the individual channels. Bars, 10  $\mu$ m.

the increase in cell numbers of heterotrophic nitrate-reducing strains caused by the presence of the organic substrate (Fig. 6B, D, and F). The surfaces of these cells were also not covered with Fe mineral particles. The surfaces of some bacteria under these mixotrophic conditions appeared rougher than the smooth surfaces of other cells in the same culture, but we observed the same morphology when we cultivated culture KS



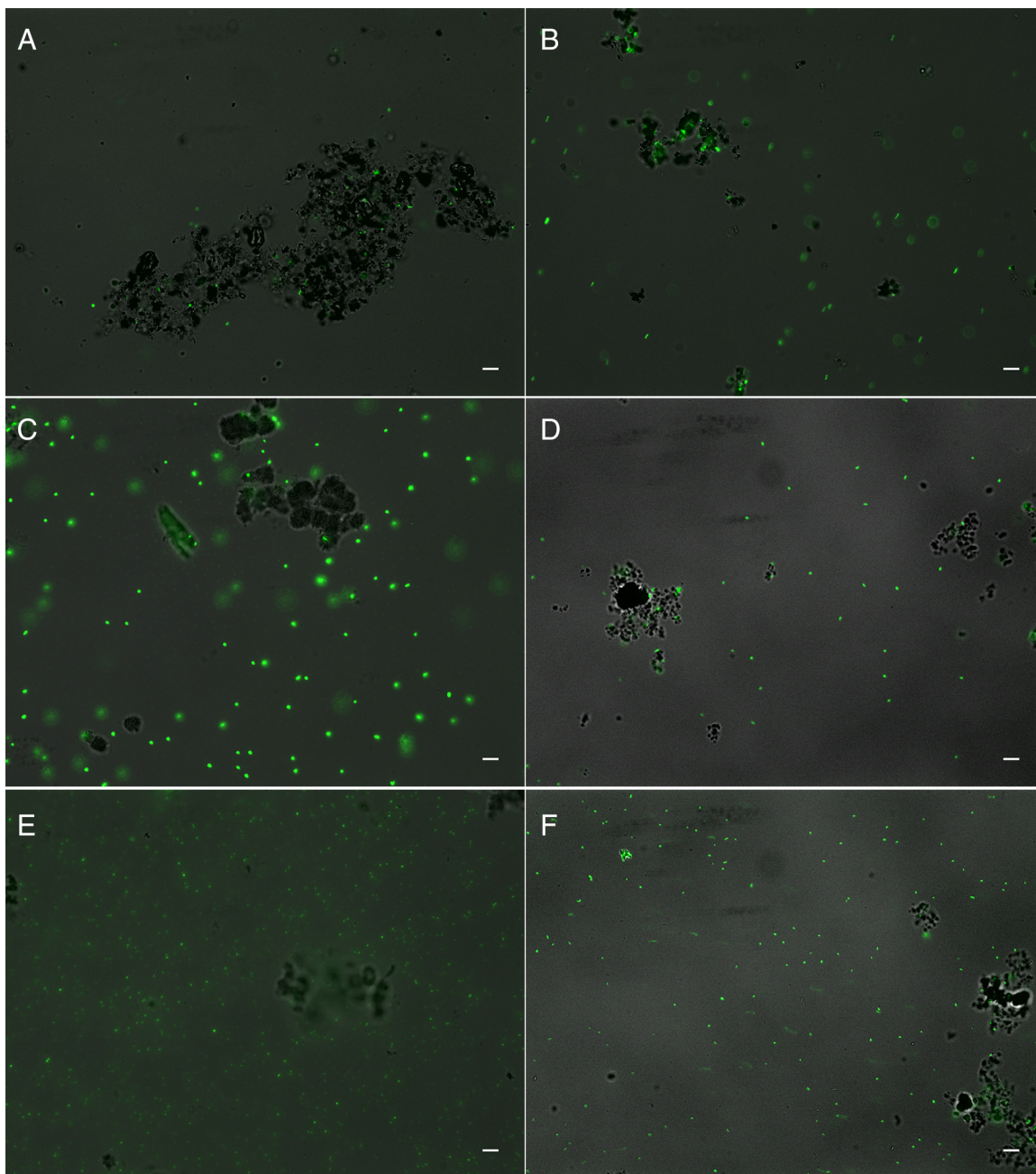


**FIG 5** Fluorescence microscopy overview images showing distribution of “planktonic” and mineral-associated cells. DNA was stained with Syto 9 (green). (A and B) Culture KS under autotrophic (4 days of incubation) (A) and mixotrophic (7 days of incubation) (B) conditions. (C and D) *Nocardioides* sp. under mixotrophic conditions (14 days of incubation) with 5 (C) and 10 (D) mM Fe(II). (E and F) *Rhodanobacter* sp. under mixotrophic conditions (14 days of incubation) with 5 (E) and 10 (F) mM Fe(II). Bars, 10  $\mu$ m.

under purely heterotrophic conditions (5 mM acetate and 4 mM nitrate [see Fig. S1 in the supplemental material]). We also confirmed the absence of Fe mineral particles on the cell surfaces under autotrophic and mixotrophic conditions using backscattered electron (BSE) imaging on the scanning electron microscope (SEM) (Fig. S2). We further analyzed the cell surfaces in pure cultures of the *Nocardioides* sp. and *Rhodanobacter* sp., which were isolated from culture KS and cultivated under mixotrophic growth conditions in setups with 5 and 10 mM Fe(II) (Fig. 8). At a 5 mM Fe(II) concentration, we found some mineral particles on most cells of the *Nocardioides* sp. (Fig. 8A to D) and on some cells of the *Rhodanobacter* sp. (Fig. 8G to J). At 10 mM Fe(II), we found that cells of both strains (*Nocardioides* and *Rhodanobacter*) were covered with some mineral

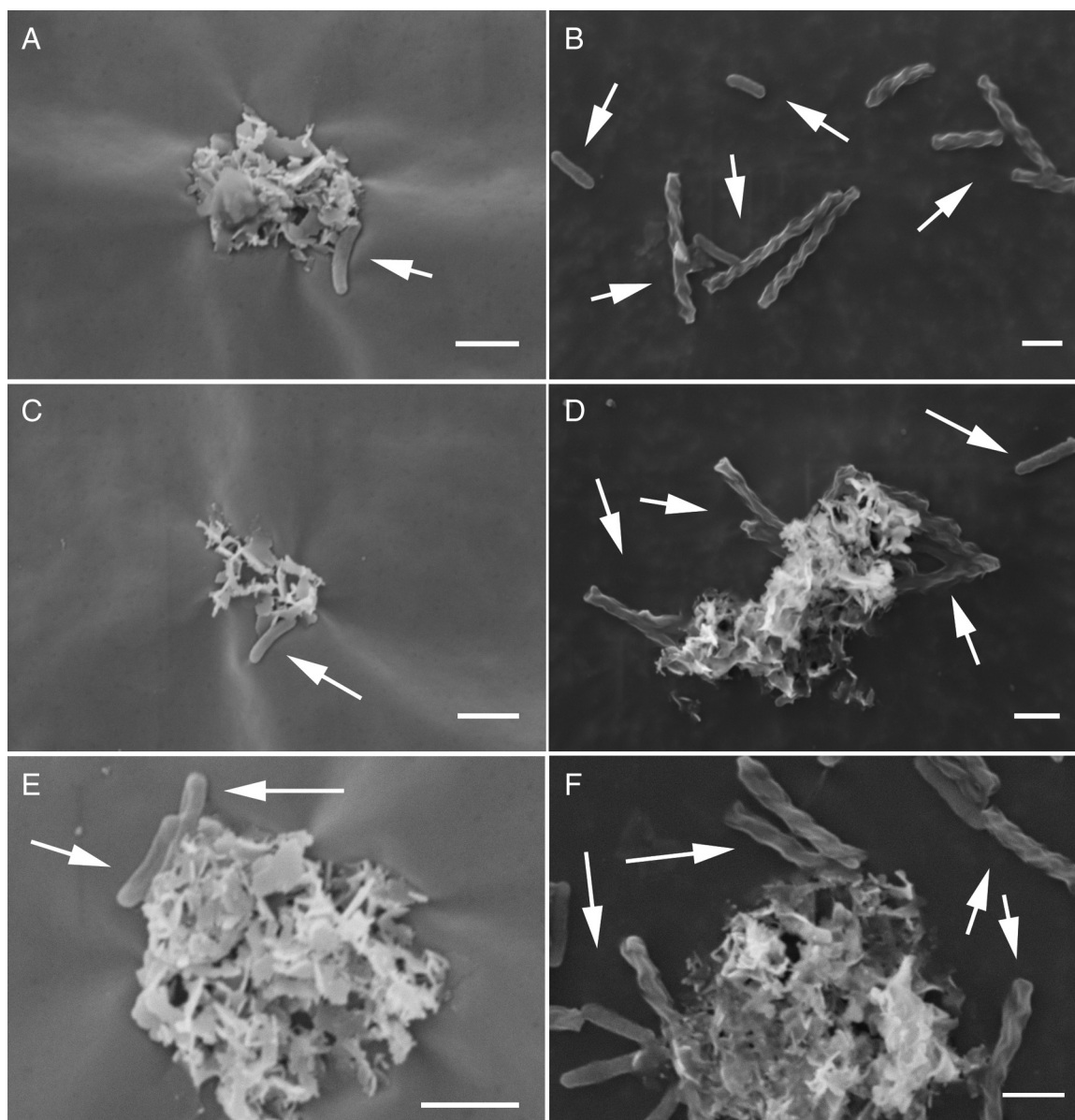


**FIG 6** SEM images of culture KS grown under autotrophic conditions (4 days of incubation) (A, C, and E) and mixotrophic conditions (7 days of incubation) (B, D, and F). White arrows indicate cells. Bars, 10  $\mu\text{m}$ .

particles and we also frequently observed more heavily encrusted cells (50 to 60% [Fig. 8E, F, K, and L]). We confirmed the presence of Fe mineral particles on cell surfaces of the *Nocardioides* sp. and *Rhodanobacter* sp. using BSE imaging on the SEM (Fig. S2).

**Mineralogy.** We used Mossbauer spectroscopy to identify the Fe minerals formed in culture KS under autotrophic and mixotrophic growth conditions (Fig. 9A and C) and also in pure cultures of *Nocardioides* sp. and *Rhodanobacter* sp. isolated from culture KS cultivated under mixotrophic growth conditions (Fig. 9B and D). Since we used unfiltered medium to be able to compare our results to previous studies of culture KS, we observed precipitation of the Fe(II) phosphate mineral vivianite upon addition of Fe(II) to the growth medium in all cases [stemming from the added Fe(II) and phosphate present in the growth medium] (Fig. 9). Since the vivianite formed during preparation of the medium before the cells are added and therefore was present in all experiments, i.e., in the KS cultures as well as in the experiments with the individual cultures, we do not expect this to influence the results. Since there was less Fe(II) oxidation in the *Rhodanobacter* and *Nocardioides* cultures, the spectra show a higher relative amount of

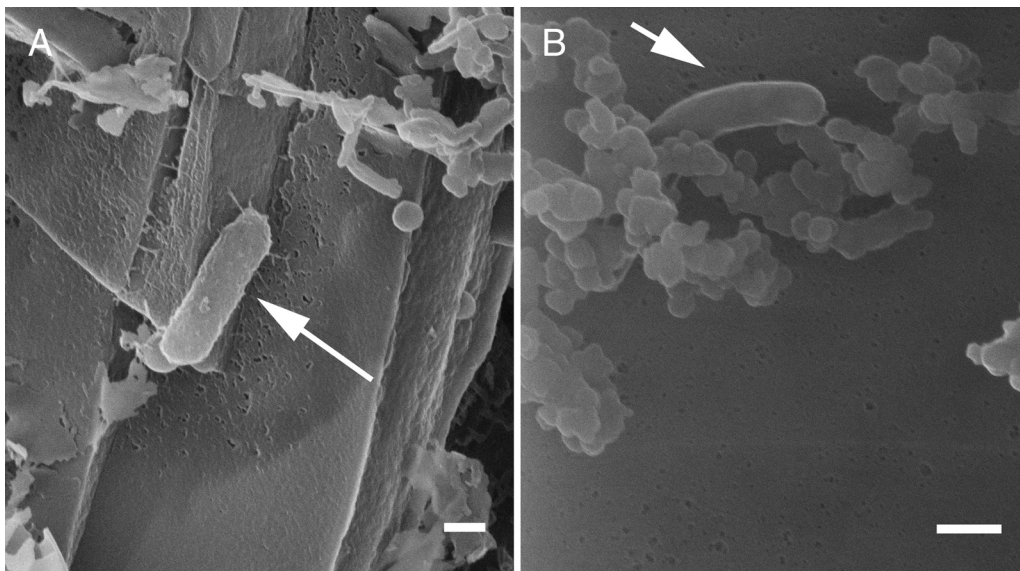


**FIG 7** Helium ion microscopy images of culture KS under autotrophic conditions (4 days of incubation). Samples were prepared either with hexamethyldisilazane (HMDS) (A) or by critical point drying (CPD) (B). White arrows indicate cells. Bars, 200 nm.

vivianite than that in culture KS. Furthermore, we identified a short-range ordered Fe(III) mineral phase which was most likely ferrihydrite in culture KS under both autotrophic and mixotrophic growth conditions at the end of Fe(II) oxidation in addition to vivianite (Fig. 9, left). In the pure cultures of the *Nocardioides* sp. and *Rhodanobacter* sp. strains, green rust was formed under mixotrophic growth conditions when ca. 4.4 mM and 4.3 mM amounts of the initially present 9.3 and 9.6 mM concentrations were oxidized to Fe(III), respectively (Fig. 9B and D).

## DISCUSSION

**EPS production and cell-mineral associations.** We found EPS closely associated with the Fe minerals formed in all analyzed cultures. Similar observations were made for the autotrophic phototrophic Fe(II) oxidizers *Rhodovulum iodosum* (41) and *Rhodobacter ferrooxidans* SW2 (42) and for the mixotrophic nitrate-reducing Fe(II)-oxidizing *Acidovorax* strain BoFeN1 (35, 39). It has been suggested that EPS is produced as a stress reaction to bind toxic Fe(II) which was present at high concentrations in our cultures or to protect the bacterial cells from encrustation (35).

Under autotrophic growth conditions, most cells present in our culture KS (approximately 96%) belong to *Gallionellaceae* sp., the designated autotrophic Fe(II) oxidizer, while the other strains account for 4% (31) (Tominski et al., unpublished). Under these autotrophic growth conditions, most of the cells were associated with mineral particles (but not encrusted [see below]). Similar associations were observed for the nonencrusting autotrophic phototrophic Fe(II)-oxidizing bacteria (41, 43) as well as for encrusting cells of the mixotrophic nitrate-reducing Fe(II)-oxidizing strain *Acidovorax* sp. BoFeN1 (35, 39). For culture KS under mixotrophic growth conditions, we observed an increase in the number of cells associated with mineral particles and in the distinguishable cell morphologies of these cells compared to those under autotrophic conditions. The number of “planktonic” cells that were not associated with minerals also increased under mixotrophic compared to autotrophic conditions, due to growth and thus an increasing abundance of heterotrophic strains from 4% under autotrophic conditions to 80 to 95% under mixotrophic conditions (Tominski et al., unpublished). Catalyzed reporter deposition fluorescence *in situ* hybridization analyses showed that the *Gallionellaceae* sp. maintains the same morphology under the two growth conditions (Tominski et al., unpublished). This suggests that under mixotrophic growth conditions cells of the other heterotrophic strains are also associated with mineral particles.

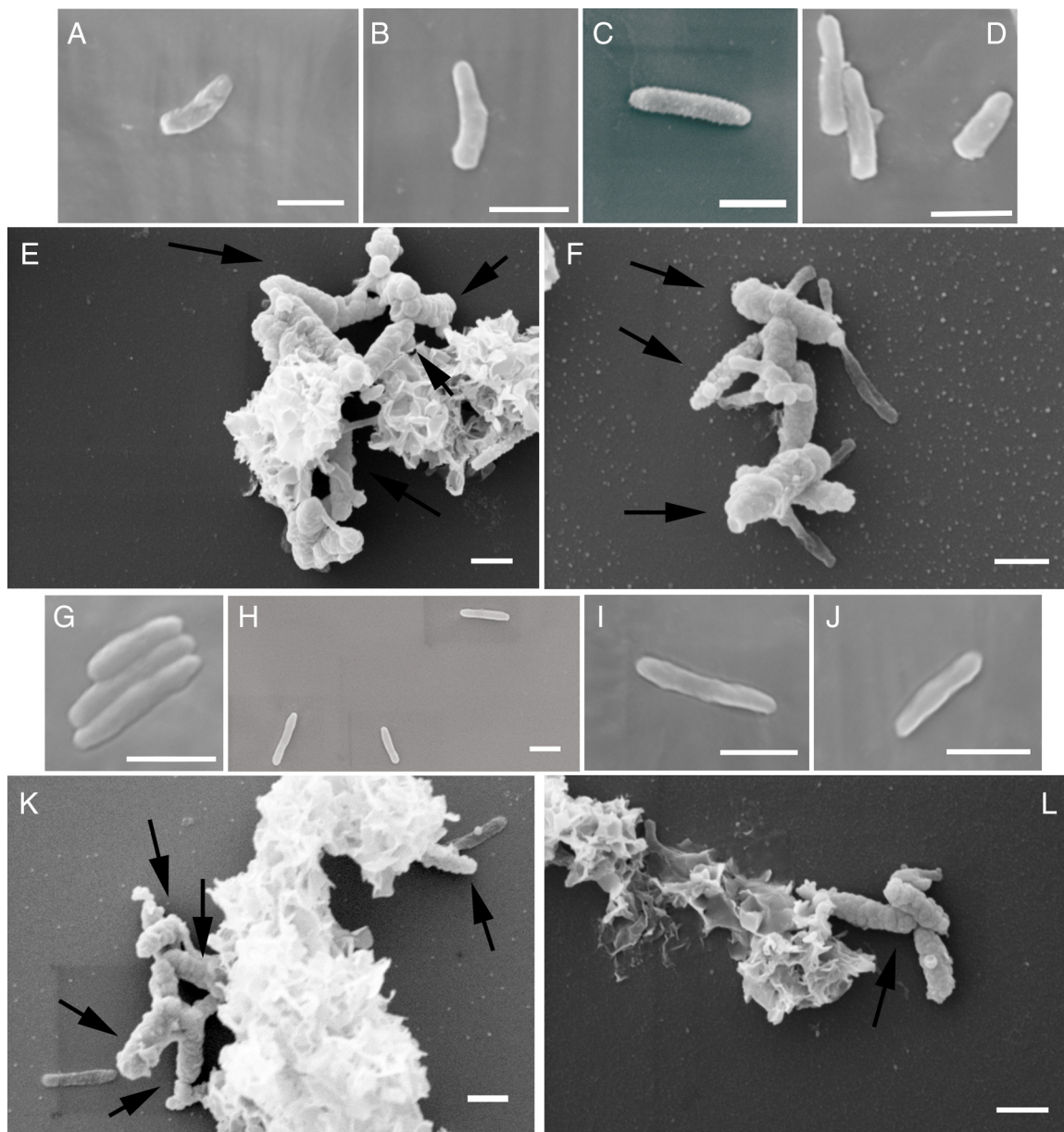


**FIG 8** SEM images of *Nocardioides* sp. (A to F) and *Rhodanobacter* sp. (G to L) isolated from culture KS grown under mixotrophic conditions (14 days of incubation) with 5 (A to D and G to J) or 10 (E, F, K, and L) mM Fe(II). Black arrows indicate encrusted cells. Bars, 10  $\mu$ m.

Metabolic interactions between the cells of the other heterotrophic strains and cells of the *Gallionellaceae* sp. strain could be one reason for their association with mineral particles, but these heterotrophic cells could also be simply associated with the mineral surface due to electrostatic interactions or because of access to mineral-associated nutrients, e.g., phosphate or trace metals (44).

**Insights from the absence of cell encrustation into mechanisms of nitrate-reducing Fe(II) oxidation in the autotrophic culture KS.** Despite the observed cell-mineral associations, during autotrophic growth of culture KS, we did not observe any cells that were encrusted in Fe minerals. This is in contrast to the reported heavy encrustation of mixotrophic nitrate-reducing Fe(II)-oxidizing bacteria and heterotrophic nitrate-reducing bacteria in the presence of high Fe(II) concentrations (3, 13, 38, 39). For most of these cultures that show encrustation, it has been suggested that abiotic oxidation of Fe(II) by accumulated nitrite formed during nitrate reduction is responsible for at least some, if not all, of the Fe(II) oxidation (35, 40). No accumulation of nitrite was

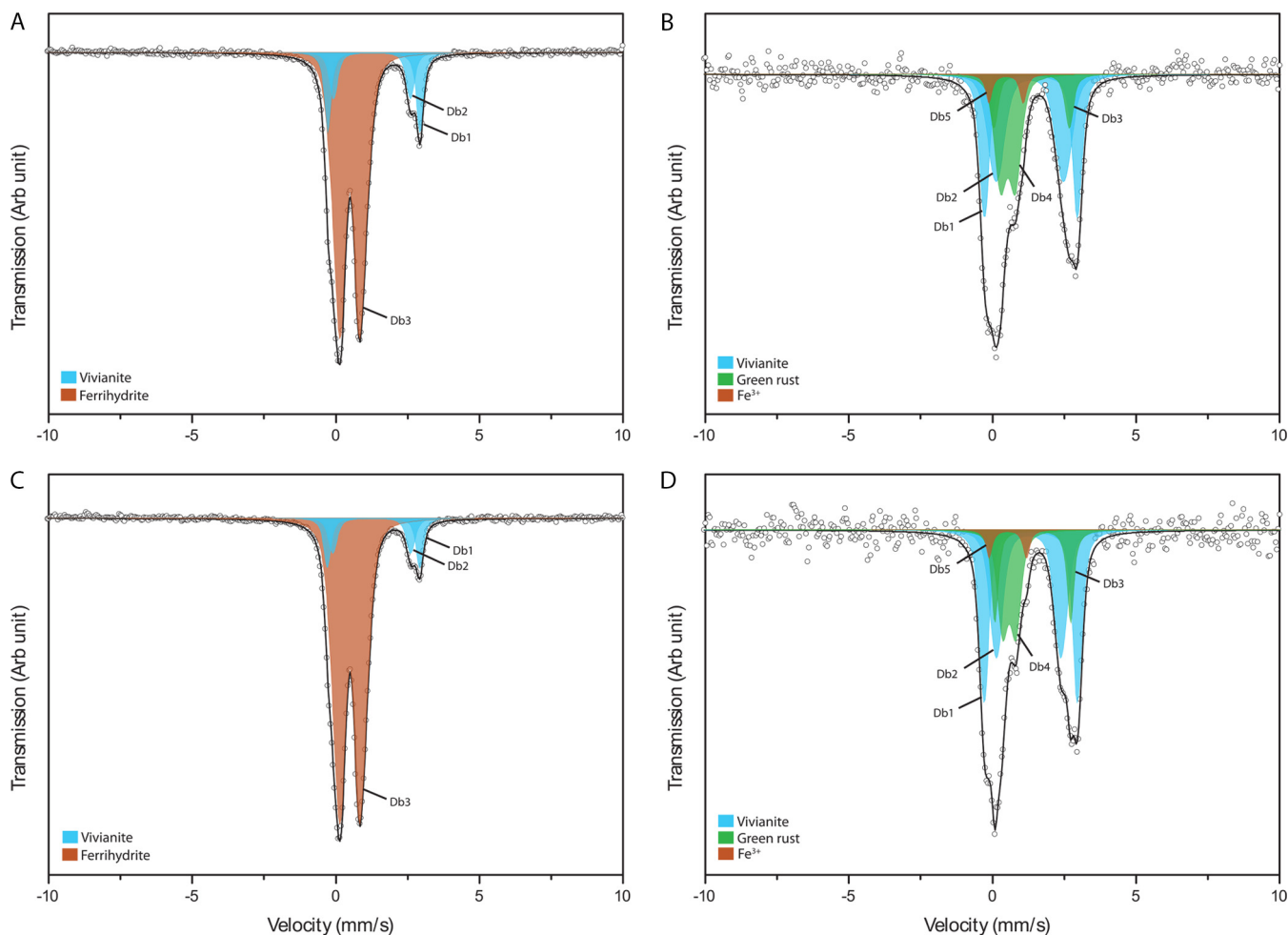


**FIG 9** Mossbauer spectra of the minerals formed by culture KS under autotrophic (A) and mixotrophic (C) conditions and by *Nocardioides* sp. (B) and *Rhodanobacter* sp. (D) under mixotrophic conditions.

observed in culture KS during autotrophic growth (10). Since culture KS can be cultivated continuously under autotrophic conditions with Fe(II) and nitrate without organic cosubstrates, Fe(II) oxidation has to be enzymatic and coupled via nitrate reduction to energy generation. Therefore, an explanation for the absence of encrusted cells in culture KS during autotrophic growth, similarly to autotrophic phototrophic and microaerophilic Fe(II) oxidizers, is that a controlled enzymatic Fe(II) oxidation and Fe(III) release mechanism prevents encrustation. Such a mechanism could allow the bacteria to prevent Fe(III) precipitation adjacent to the cell, while the abiotic oxidation of Fe(II) by nitrite observed for mixotrophic and heterotrophic nitrate reducers (35) does not allow control over the location of Fe(III) precipitation and even takes place in the periplasm, where the nitrite is present (45). It has to be noted, however, that encrustation has also been observed in some bacteria that were reported as autotrophic nitrate-reducing Fe(II) oxidizers, but it remains unclear whether these strains are indeed autotrophic (19, 20, 22, 46).

**Dependency of encrustation on Fe(II) and nitrite concentrations.** The low abundance (ca. 4%) of the other strains present in culture KS compared to the dominating *Gallionellaceae* sp. (96%) under autotrophic conditions and the strong increase of their abundance (80 to 95%) under mixotrophic growth conditions suggest that they carry out heterotrophic and potentially also mixotrophic nitrate reduction with acetate and acetate/Fe(II), respectively. Therefore, encrustation of these strains in the presence of high Fe(II) concentrations (10 mM) under mixotrophic conditions, caused by nitrite

formed during heterotrophic nitrate reduction, as reported by Klueglein et al. (35), seemed likely. Surprisingly, we did not observe such encrustation of any cells, and no nitrite accumulation was observed in mixotrophic incubations of culture KS (Tominski et al., unpublished). In contrast, in mixotrophic pure cultures of the *Nocardioides* sp. and *Rhodanobacter* sp. (isolated from culture KS), nitrite accumulated and mineral-covered cell surfaces and encrusted cells were frequently observed in the presence of 10 mM Fe(II). The smaller amount of mineral particles on the cell surfaces of the isolates at 5 mM than at 10 mM Fe(II) suggests that the extent of encrustation caused by indirect Fe(II) oxidation by reactive nitrogen species during heterotrophic nitrate reduction does depend on Fe(II) concentrations as suggested before (3). The absence of nitrite and therefore the absence of uncontrolled abiotic Fe(II) oxidation in culture KS under mixotrophic conditions could prevent encrustation. However, it remains unclear why nitrite does not accumulate in culture KS under mixotrophic conditions despite the high abundance of heterotrophic nitrate reducers, in contrast to mixotrophic incubations of pure cultures of the *Nocardioides* sp. and *Rhodanobacter* sp. and other nitrate reducers (35).

**Possible metabolic interactions between different strains in culture KS.** Metabolic interactions between the several bacterial strains present in culture KS could prevent accumulation of nitrite and promote complete denitrification under both mixotrophic and autotrophic Fe(II)-oxidizing growth conditions. A recent metagenomic study of culture KS (31) found all genes necessary for complete denitrification in both *Rhodanobacter* sp. and *Bradyrhizobium* sp., while in *Gallionellaceae* sp. only genes for the reduction of nitrate to nitrite and nitrite to nitric oxide were found. Therefore, the *Gallionellaceae* sp. could depend on the other strains for complete denitrification under autotrophic and also mixotrophic Fe(II)-oxidizing conditions to avoid potential toxic effects of accumulating nitric oxide (47). However, this would require the transfer of nitric oxide through the Fe(II)-containing growth medium, since the cells of *Gallionellaceae* sp. outnumber other bacteria under autotrophic conditions. A transfer of nitric oxide would on the one hand explain why we did not detect any accumulating nitrite under both autotrophic and mixotrophic conditions in culture KS, in contrast to the pure cultures of the *Nocardioides* sp. and *Rhodanobacter* sp. under mixotrophic conditions. On the other hand, it would also explain the absence of abiotic Fe(II) oxidation under these conditions, since oxidation of Fe(II) by free nitric oxide depends on the availability of mineral surfaces as catalyst, and therefore, in particular, in the beginning of nitrate reduction and Fe(II) oxidation, the abiotic reaction does not play an important role.

Additionally, it is possible that the competition among the several strains in culture KS promotes more efficient denitrification without accumulation of nitrite. It has also been suggested previously that *Gallionellaceae* sp. could supply the other bacteria with organic substrates under autotrophic conditions in the form of released EPS (31). The detection of EPS in this study confirms this possibility of cross-feeding between the Fe(II) oxidizer and the heterotrophs. Finally, the fact that isolation of the *Gallionellaceae* sp. from culture KS as an autotrophic Fe(II)-oxidizing pure culture was, so far, not possible, strongly argues for some dependencies between bacterial strains in culture KS for nitrate-reducing Fe(II) oxidation. While the underlying mechanism is not fully clear, it appears that the presence of several bacterial strains in culture KS promotes denitrification without accumulation of nitrite and thus prevents abiotic Fe(II) oxidation and cell encrustation.

**Formation of green rust or ferrihydrite depending on Fe(II) oxidation mechanisms.** Ferrihydrite was shown to be formed as the Fe(III) mineral product by autotrophic microaerophilic (48) and autotrophic phototrophic (41, 49, 50) Fe(II) oxidizers. In some cases, this initial ferrihydrite formation was followed by slow, Fe(II)-induced goethite formation (51), whereas in the mixotrophic nitrate-reducing Fe(II) oxidizer BoFeN1, where Fe(II) is probably oxidized by the nitrite formed during heterotrophic nitrate reduction, green rust as an intermediate and goethite as a final product have

been described (9, 40, 45, 52, 53). It has also been demonstrated that direct abiotic oxidation of Fe(II) by nitrite can produce green rust (54). We observed a similar green rust formation in the present study in mixotrophic pure cultures of *Nocardioides* sp. and *Rhodanobacter* sp. isolated from culture KS, where nitrite accumulated and Fe(II) was oxidized incompletely (28 to 45% only), probably abiotically by the formed nitrite. Minerals of a greenish color were also observed previously by others in pure cultures of other isolates from culture KS that were not capable of autotrophic Fe(II) oxidation coupled to nitrate reduction, even though the identity of these minerals was not determined (30). Therefore, almost complete Fe(II) oxidation and formation of ferrihydrite in culture KS under autotrophic conditions are another hint of enzymatic Fe(II) oxidation. It is possible that Fe(II) is also mainly oxidized by enzymatic Fe(II) oxidation coupled to nitrate reduction by the *Gallionellaceae* sp. under mixotrophic conditions, since formation of ferrihydrite and almost complete Fe(II) oxidation were also observed under these conditions. In summary, these data suggest that incomplete Fe(II) oxidation and the formation of green rust as an intermediate [followed by goethite formation as final Fe(III) product] point toward a nonenzymatic Fe(II) oxidation by nitrite while rapid, almost complete Fe(II) oxidation under anoxic conditions with ferrihydrite as final Fe(III) product suggests an enzymatic Fe(II) oxidation.

**Environmental significance of encrustation.** Nitrate-reducing bacteria face encrustation in Fe(III) minerals in the presence of Fe(II), as discussed in detail by Klueglein et al. (35). Since most studies with nitrate-reducing bacteria that encrust in Fe(III) minerals were conducted using batch cultures with Fe(II) concentrations in the high (5 to 10) millimolar range (3, 9, 22, 35, 39, 46), an open question is whether such a cell encrustation also occurs in the environment where lower Fe(II) concentrations (micromolar concentrations of tens to hundreds) are common. We found that encrustation did not occur in pure cultures of *Nocardioides* sp. and *Rhodanobacter* sp. when we simply lowered the Fe(II) concentrations from 10 mM to 5 mM. A dependence of encrustation on Fe(II) concentrations and its disappearance at lower Fe(II) concentrations have also been shown for *Acidovorax* sp. strain 2AN (3). This indicates that encrustation is potentially negligible in environments that do not have elevated Fe(II) concentrations. In environments with elevated Fe(II) concentrations, bacteria encrusted in Fe minerals have been found (19, 20, 55–57). In anoxic environments, the abiotic oxidation of Fe(II) by metabolic products of denitrifying bacteria or by O<sub>2</sub> under microoxic conditions can potentially contribute to encrustation of microbial cells. However, neither high concentrations of nitrite nor encrusted bacteria were detected in culture KS under mixotrophic conditions with high Fe(II) concentrations, where many heterotrophic and potentially mixotrophic nitrate-reducing bacteria are present. This indicates that interactions occurring in a mixed bacterial community, in which bacteria are frequently found in the environment, can prevent nitrite accumulation and encrustation even in the presence of high Fe(II) concentrations. However, accumulation of nitrite can also occur in environmental microbial communities (58–61). In environments with elevated Fe(II) concentrations, this could lead to encrustation. Nevertheless, in most sedimentary or soil environments no elevated Fe(II) concentrations occur and the accumulating nitrite will not lead to encrustation, but it will affect the biogeochemical Fe cycle via the abiotic reaction of nitrite with Fe(II).

## MATERIALS AND METHODS

**Source of microorganisms.** The chemolithoautotrophic nitrate-reducing Fe(II)-oxidizing enrichment culture KS (10) was provided to Andreas Kappler by Kristina Straub in 2005 and has been maintained as a growing autotrophic culture in our laboratory since then. The enrichment culture was originally obtained from a freshwater sediment in Bremen, Germany.

**Microbial growth medium and growth conditions.** Bacteria were grown in 22 mM bicarbonate-buffered anoxic freshwater mineral medium (pH 7.0, headspace N<sub>2</sub>/CO<sub>2</sub>, 90:10 [vol/vol]) as described in reference 43, modified from the method described in reference 62. For cultivation of culture KS under autotrophic growth conditions, the medium was amended with 8 to 10 mM Fe(II) chloride as electron donor and 4 mM sodium nitrate as electron acceptor as described in reference 10. For mixotrophic growth conditions, 8 to 10 mM Fe(II) and 4 mM nitrate plus 5 mM sodium acetate were used as an additional electron donor. Medium was inoculated with 1% (vol/vol) of a preculture of culture KS grown

under autotrophic conditions and incubated in the dark at 28°C. The *Nocardioides* and *Rhodanobacter* strains were isolated from the enrichment culture KS using different solid oxalic media and a heterotrophically (5 mM acetate and 4 mM nitrate) grown preculture (Tominski et al., unpublished). Both strains were cultivated under mixotrophic growth conditions in anoxic medium amended with 5 or 10 mM Fe(II), 5 mM acetate, and 4 mM nitrate. Cultures were inoculated with 1% (vol/vol) of a preculture grown under heterotrophic conditions (5 mM acetate and 4 mM nitrate) and incubated in the dark at 28°C.

**Quantification of Fe(II), acetate, and nitrate.** Acetate was quantified by high-performance liquid chromatography as described previously (63), with an 0.25 mM detection limit. An automated continuous-flow injection analyzer (FIA) system (Seal Analytical, Germany) was used for photometric quantification of nitrate and nitrite. The system contains a dialysis membrane to remove iron and prevent side reactions of nitrate and nitrite during analysis. Hydrazine sulfate was used to reduce nitrate to nitrite, which is quantified photometrically with *N*-1-naphthyl ethylenediamine at 550 nm (40). Fe was quantified in microtiter plates with the spectrophotometric ferrozine assay (64) using a revised protocol for nitrite-containing samples (40). One hundred microliters of culture suspension was withdrawn anoxically and acidified in 900  $\mu$ l of 40 mM sulfamic acid for 1 h at room temperature. Acidification in sulfamic acid stabilizes Fe(II) and reacts with the present nitrite that otherwise would cause additional abiotic Fe(II) oxidation. The ferrozine-Fe(II) complex was quantified at 562 nm with a spectrophotometric plate reader (Multiskan GO; Thermo Fisher Scientific, USA). Measurements were performed in triplicates.

**Mossbauer spectroscopy.** Samples were taken by filtration from the culture bottles using syringe filters in an anoxic glove box. The sampled minerals were frozen and stored anoxically until measurements were taken. The samples were inserted into a closed-cycle exchange gas cryostat (Janis Cryogenics). The spectra were recorded at 77 K in transmission geometry using a constant acceleration drive system (WissEL). A  $^{57}\text{Co}$  source embedded in a rhodium matrix was used as a gamma radiation source. The sample spectra were calibrated against a 7- $\mu$ m-thick  $\alpha$ - $^{57}\text{Fe}$  foil at room temperature (RT). The RECOL software suite (University of Ottawa, Canada) was used for the calibration and the modeling of the spectra. The spectra were modeled using Voigt-based line shapes. The Lorentz half-width-half-maximum (HWHM) value was kept constant at 0.133 mm/s (determined from the minimum line width of the 3 and 4 peaks of the calibration foil) in the models, and the sigma ( $\sigma$ ) parameter was used to account for line broadening until the fitting was acceptable. The sample spectra were analyzed in respect to the center shift (CS) values and the quadrupole splitting (QS).

**Scanning electron, helium ion, fluorescence, and confocal laser scanning microscopy.** Samples for microscopic analysis were taken from the enrichment culture KS when Fe(II) was almost completely oxidized (after 7 days under mixotrophic conditions and after 4 days under autotrophic conditions). Samples from the pure cultures of *Nocardioides* and *Rhodanobacter* were taken when nitrate was almost completely consumed (i.e., after 14 days). For scanning electron microscopy (SEM), samples were fixed with 2.5% glutaraldehyde and 2% formaldehyde at 4°C overnight. In the case of the *Nocardioides* and *Rhodanobacter* strains, the growth medium was replaced by 0.1 M phosphate buffer after centrifugation for 5 min at  $5,000 \times g$  prior to fixation to prevent artifacts by abiotic oxidation of the remaining Fe(II) in the growth medium. After fixation, the samples were applied to poly-L-lysine-coated glass coverslips or Formvar-coated transmission electron microscopy (TEM) grids. After washing with 0.1 M phosphate buffer, samples were successively dehydrated using a series of ethanol dilutions (30, 70, 95, and twice 100%, ethanol dried on a molecular sieve). Samples were dried with hexamethyldisilazane (HMDS) (65, 66) and mounted on SEM stubs using conductive carbon pads. Samples were coated with 8-nm Pt and examined in a Leo 1450 VP SEM (Zeiss, Oberkochen, Germany) at 6 kV and 5-mm working distance using an Everhart-Thornley secondary electron (SE) detector. For comparative imaging, the sample surface was examined with a SE detector (6 kV) and the distribution of iron was determined with a backscattered electron (BSE) detector (12 kV) at 10-mm working distance. Being dominated by topography contrast, SE images show the topographic structure of the samples, with only a minor influence of their chemical composition. In contrast, BSE images are characterized by Z number contrast, resulting in higher brightness from areas with a higher average atomic number. Therefore, in BSE mode the signal for iron is much stronger than the carbon signal due to the difference in their Z number and organic particles, and cells almost disappear from the BSE images unless iron is present on the cell surface or in the periplasm.

For He ion microscopy (HIM), a sample grown under standard conditions was fixed with glutaraldehyde (2.5% final concentration) and left at 4°C overnight. Dehydration was performed by an ethanol dilution series with increasing ethanol concentrations (30%, 75%, 95% and twice 100%). Samples were then treated with hexamethyldisilazane (HMDS; Sigma-Aldrich, St. Louis, MO, USA) and dried at room temperature or by critical point drying (CPD). HIM was performed with a Zeiss Orion Plus HIM (Carl Zeiss, Peabody, MA).

Fluorescence and confocal laser scanning microscopy (CLSM) samples were prepared carefully in an anoxic glove box with minimal handling to avoid shear stress and to preserve the cell-mineral associations. Culture bottles were gently mixed prior to sampling. Two-hundred-microliter sample aliquots were carefully withdrawn with syringes and cannulas of 1.2-mm diameter. For fluorescence microscopy, samples were stained with Syto 9 (Molecular Probes, Carlsbad, CA; 1.22  $\mu$ M final concentration) for 5 min. For confocal microscopy, stains were applied sequentially: first Syto 9 (Molecular Probes, Carlsbad, CA; 1.22  $\mu$ M final concentration) for 5 min and then peanut agglutinin (PNA)-Alexa Fluor 647 conjugate (Molecular Probes, Carlsbad, CA; 8.58- $\mu$ g/ml final concentration) for 30 min. Low concentrations of all dyes were used to avoid potential unspecific binding. Samples were spotted onto microscopy slides, topped with cover glasses, and sealed with nail polish. Samples were gently mixed using Pasteur pipettes with wide openings after application of each stain and prior to spotting onto microscopy slides. For



fluorescence microscopy, a Leica DM 5500 B epifluorescence microscope equipped with a 40× air objective (numerical aperture [NA] 0.75) was used. CLSM measurements were performed on a Leica SPE confocal laser scanning microscope equipped with an ACS Apo 63 × water immersion objective (NA 1.15). Syto 9 was excited with a 488-nm laser, and emission was recorded between 500 nm and 600 nm. The PNA-Alexa Fluor 647 conjugate was excited with a 635-nm laser, and emission was recorded between 647 nm and 780 nm. Minerals were recorded using their reflection signal of the 488-nm laser.

## SUPPLEMENTAL MATERIAL

Supplemental material for this article may be found at <https://doi.org/10.1128/AEM.00752-17>.

**SUPPLEMENTAL FILE 1**, PDF file, 1.0 MB.

## ACKNOWLEDGMENTS

We thank Ellen Struve for FIA and high-performance liquid chromatography measurements, Likai Hao for help with CLSM sample preparation, and Hartmut Schulz for help with electron microscopy analysis. We are grateful for using the analytical facilities of the Centre for Chemical Microscopy (ProVIS) at the Helmholtz Centre for Environmental Research. In particular, we thank Matthias Schmidt, who carried out the scanning helium ion microscopy.

A. Kappler and M. Nordhoff were supported by the European Research Council under the European Union Seventh Framework Program (FP/2007-2013)/ERC grant agreement 307320-MICROFOX. This work was also supported by the German Research Foundation (DFG)-funded research training group RTG 1708 “Molecular principles of bacterial survival strategies” (C.T. and S.K.). The Helmholtz Centre for Environmental Research is supported by European Regional Development Funds (EFRE - Europe funds Saxony) and the Helmholtz Association.

## REFERENCES

1. Benz M, Brune A, Schink B. 1998. Anaerobic and aerobic oxidation of ferrous iron at neutral pH by chemoheterotrophic nitrate-reducing bacteria. *Arch Microbiol* 169:159–165. <https://doi.org/10.1007/s002030050555>.
2. Dubinina GA, Sorokina AY. 2014. Neutrophilic lithotrophic iron-oxidizing prokaryotes and their role in the biogeochemical processes of the iron cycle. *Mikrobiologiya* 83:127–142. (In Russian.)
3. Chakraborty A, Roden EE, Schieber J, Picardal F. 2011. Enhanced growth of *Acidovorax* sp. strain 2AN during nitrate-dependent Fe(II) oxidation in batch and continuous-flow systems. *Appl Environ Microbiol* 77:8548–8556. <https://doi.org/10.1128/AEM.06214-11>.
4. Hafenbradl D, Keller M, Dirmeier R, Rachel R, Rosznagel P, Burggraf S, Huber H, Stetter KO. 1996. *Ferroglobus placidus* gen nov, sp nov, a novel hyperthermophilic archaeum that oxidizes Fe<sup>2+</sup> at neutral pH under anoxic conditions. *Arch Microbiol* 166:308–314. <https://doi.org/10.1007/s002030050388>.
5. Kumaraswamy R, Sjollem K, Kuenen G, van Loosdrecht M, Muyzer G. 2006. Nitrate-dependent [Fe(II)EDTA]<sub>2</sub>-oxidation by *Paracoccus ferrooxidans* sp. nov., isolated from a denitrifying bioreactor. *Syst Appl Microbiol* 29:276–286. <https://doi.org/10.1016/j.syapm.2005.08.001>.
6. Lack JG, Chaudhuri SK, Chakraborty R, Achenbach LA, Coates JD. 2002. Anaerobic biooxidation of Fe(II) by *Dechlorosoma suillum*. *Microb Ecol* 43:424–431. <https://doi.org/10.1007/s00248-001-1061-1>.
7. Weber K, Hedrick D, Peacock A, Thrash JC, White D, Achenbach L, Coates J. 2009. Physiological and taxonomic description of the novel autotrophic, metal oxidizing bacterium, *Pseudogulbenkiania* sp. strain 2002. *Appl Microbiol Biotechnol* 83:555–565. <https://doi.org/10.1007/s00253-009-1934-7>.
8. Shelobolina ES, Konishi H, Xu H, Benzine J, Xiong MY, Wu T, Blöthe M, Roden E. 2012. Isolation of phyllosilicate-iron redox cycling microorganisms from an illite-smectite rich hydromorphic soil. *Front Microbiol* 3:134. <https://doi.org/10.3389/fmicb.2012.00134>.
9. Kappler A, Schink B, Newman DK. 2005. Fe(III) mineral formation and cell encrustation by the nitrate-dependent Fe(II)-oxidizer strain BoFeN1. *Geobiology* 3:235–245. <https://doi.org/10.1111/j.1472-4669.2006.00056.x>.
10. Straub KL, Benz M, Schink B, Widdel F. 1996. Anaerobic, nitrate-dependent microbial oxidation of ferrous iron. *Appl Environ Microbiol* 62:1458–1460.
11. Muehe EM, Gerhardt S, Schink B, Kappler A. 2009. Ecophysiology and the energetic benefit of mixotrophic Fe(II) oxidation by various strains of nitrate-reducing bacteria. *FEMS Microbiol Ecol* 70:335–343. <https://doi.org/10.1111/j.1574-6941.2009.00755.x>.
12. Chakraborty A, Picardal F. 2013. Induction of nitrate-dependent Fe(II) oxidation by Fe(II) in *Dechloromonas* sp. strain UWNR4 and *Acidovorax* sp. strain 2AN. *Appl Environ Microbiol* 79:748–752. <https://doi.org/10.1128/AEM.02709-12>.
13. Straub KL, Schönhuber WA, Buchholz-Cleven BEE, Schink B. 2004. Diversity of ferrous iron-oxidizing, nitrate-reducing bacteria and their involvement in oxygen-independent iron cycling. *Geomicrobiol J* 21:371–378. <https://doi.org/10.1080/01490450490485854>.
14. Weber KA, Achenbach LA, Coates JD. 2006. Microorganisms pumping iron: anaerobic microbial iron oxidation and reduction. *Nat Rev Microbiol* 4:752–764. <https://doi.org/10.1038/nrmicro1490>.
15. Straub KL, Buchholz-Cleven BEE. 1998. Enumeration and detection of anaerobic ferrous iron-oxidizing, nitrate-reducing bacteria from diverse European sediments. *Appl Environ Microbiol* 64:4846–4856.
16. Chaudhuri SK, Lack JG, Coates JD. 2001. Biogenic magnetite formation through anaerobic biooxidation of Fe(II). *Appl Environ Microbiol* 67:2844–2848. <https://doi.org/10.1128/AEM.67.6.2844-2848.2001>.
17. Coates JD, Chakraborty R, Lack JG, O'Connor SM, Cole KA, Bender KS, Achenbach LA. 2001. Anaerobic benzene oxidation coupled to nitrate reduction in pure culture by two strains of *Dechloromonas*. *Nature* 411:1039–1043. <https://doi.org/10.1038/35082545>.
18. Byrne-Bailey KG, Weber KA, Chair AH, Bose S, Knox T, Spanbauer TL, Chertkov O, Coates JD. 2010. Completed genome sequence of the anaerobic iron-oxidizing bacterium *Acidovorax ebreus* strain TPSY. *J Bacteriol* 192:1475–1476. <https://doi.org/10.1128/JB.01449-09>.
19. Sorokina AY, Chernousova EY, Dubinina GA. 2012. *Hoefflea siderophila* sp. nov., a new neutrophilic iron-oxidizing bacterium. *Microbiology* 81:59–66. <https://doi.org/10.1134/S0026261712010146>.
20. Sorokina AY, Chernousova EY, Dubinina GA. 2012. *Ferrovibrio denitrificans* gen. nov., sp. nov., a novel neutrophilic facultative anaerobic

- Fe(II)-oxidizing bacterium. *FEMS Microbiol Lett* 335:19–25. <https://doi.org/10.1111/j.1574-6968.2012.02631.x>.
21. Weber KA, Pollock J, Cole KA, O'Connor SM, Achenbach LA, Coates JD. 2006. Anaerobic nitrate-dependent iron(II) bio-oxidation by a novel lithoautotrophic betaproteobacterium, strain 2002. *Appl Environ Microbiol* 72:686–694. <https://doi.org/10.1128/AEM.72.1.686-694.2006>.
  22. Mattes A, Gould D, Taupp M, Glasauer S. 2013. A novel autotrophic bacterium isolated from an engineered wetland system links nitrate-coupled iron oxidation to the removal of As, Zn and S. *Water Air Soil Pollut* 224:1490. <https://doi.org/10.1007/s11270-013-1490-8>.
  23. Finneran KT, Housewright ME, Lovley DR. 2002. Multiple influences of nitrate on uranium solubility during bioremediation of uranium-contaminated subsurface sediments. *Environ Microbiol* 4:510–516. <https://doi.org/10.1046/j.1462-2920.2002.00317.x>.
  24. Su JF, Shao SC, Huang TL, Ma F, Yang SF, Zhou ZM, Zheng SC. 2015. Anaerobic nitrate-dependent iron(II) oxidation by a novel autotrophic bacterium, *Pseudomonas* sp. SZF15. *J Environ Chem Eng* 3:2187–2193. <https://doi.org/10.1016/j.jece.2015.07.030>.
  25. Benzine J, Shelobolina E, Xiong MY, Kennedy DW, McKinley JP, Lin XJ, Roden EE. 2013. Fe-phylosilicate redox cycling organisms from a redox transition zone in Hanford 300 Area sediments. *Front Microbiol* 4:388. <https://doi.org/10.3389/fmicb.2013.00388>.
  26. Shelobolina ES, Vanpraagh CG, Lovley DR. 2003. Use of ferric and ferrous iron containing minerals for respiration by *Desulfotobacterium frappierii*. *Geomicrobiol J* 20:143–156. <https://doi.org/10.1080/01490450303884>.
  27. Li BH, Tian CY, Zhang DY, Pan XL. 2014. Anaerobic nitrate-dependent iron(II) oxidation by a novel autotrophic bacterium, *Citrobacter freundii* strain PXL1. *Geomicrobiol J* 31:138–144. <https://doi.org/10.1080/01490451.2013.816393>.
  28. Zhou J, Wang H, Yang K, Ji B, Chen D, Zhang H, Sun Y, Tian J. 2016. Autotrophic denitrification by nitrate-dependent Fe(II) oxidation in a continuous up-flow biofilter. *Bioprocess Biosyst Eng* 39:277–284. <https://doi.org/10.1007/s00449-015-1511-7>.
  29. Laufer K, Røy H, Jørgensen BB, Kappler A. 2016. Evidence for the existence of autotrophic nitrate-reducing Fe(II)-oxidizing bacteria in marine coastal sediment. *Appl Environ Microbiol* 82:6120–6131. <https://doi.org/10.1128/aem.01570-16>.
  30. Blothe M, Roden EE. 2009. Composition and activity of an autotrophic Fe(II)-oxidizing, nitrate-reducing enrichment culture. *Appl Environ Microbiol* 75:6937–6940. <https://doi.org/10.1128/AEM.01742-09>.
  31. He S, Tominski C, Kappler A, Behrens S, Roden EE. 2016. Metagenomic analyses of the autotrophic Fe(II)-oxidizing, nitrate-reducing enrichment culture KS. *Appl Environ Microbiol* 82:2656–2668. <https://doi.org/10.1128/AEM.03493-15>.
  32. Weber KA, Picardal FW, Roden EE. 2001. Microbially catalyzed nitrate-dependent oxidation of biogenic solid-phase Fe(II) compounds. *Environ Sci Technol* 35:1644–1650. <https://doi.org/10.1021/es0016598>.
  33. Shelobolina E, Xu HF, Konishi H, Kukkadapu R, Wu T, Blothe M, Roden E. 2012. Microbial lithotrophic oxidation of structural Fe(II) in biotite. *Appl Environ Microbiol* 78:5746–5752. <https://doi.org/10.1128/AEM.01034-12>.
  34. Schädler S, Burkhardt C, Hegler F, Straub KL, Miot J, Benzerara K, Kappler A. 2009. Formation of cell-iron-mineral aggregates by phototrophic and nitrate-reducing anaerobic Fe(II)-oxidizing bacteria. *Geomicrobiol J* 26:93–103. <https://doi.org/10.1080/01490450802660573>.
  35. Klueglein N, Zeitvogel F, Stierhof Y-D, Floetenmeyer M, Konhauser KO, Kappler A, Obst M. 2014. Potential role of nitrite for abiotic Fe(II) oxidation and cell encrustation during nitrate reduction by denitrifying bacteria. *Appl Environ Microbiol* 80:1051–1061. <https://doi.org/10.1128/AEM.03277-13>.
  36. Hegler F, Schmidt C, Schwarz H, Kappler A. 2010. Does a low-pH microenvironment around phototrophic Fe(II)-oxidizing bacteria prevent cell encrustation by Fe(III) minerals? *FEMS Microbiol Ecol* 74:592–600. <https://doi.org/10.1111/j.1574-6941.2010.00975.x>.
  37. Miot J, Benzerara K, Obst M, Kappler A, Hegler F, Schädler S, Bouchez C, Guyot F, Morin G. 2009. Extracellular iron biomineralization by photoautotrophic iron-oxidizing bacteria. *Appl Environ Microbiol* 75:5586–5591. <https://doi.org/10.1128/AEM.00490-09>.
  38. Saini G, Chan CS. 2013. Near-neutral surface charge and hydrophilicity prevent mineral encrustation of Fe-oxidizing micro-organisms. *Geobiology* 11:191–200. <https://doi.org/10.1111/gbi.12021>.
  39. Schmid G, Zeitvogel F, Hao L, Ingino P, Floetenmeyer M, Stierhof YD, Schroepel B, Burkhardt CJ, Kappler A, Obst M. 2014. 3-D analysis of bacterial cell-(iron) mineral aggregates formed during Fe(II) oxidation by the nitrate-reducing *Acidovorax* sp. strain BoFeN1 using complementary microscopy tomography approaches. *Geobiology* 12:340–361. <https://doi.org/10.1111/gbi.12088>.
  40. Klueglein N, Kappler A. 2013. Corrigendum. Abiotic oxidation of Fe(II) by reactive nitrogen species in cultures of the nitrate-reducing Fe(II) oxidizer *Acidovorax* sp. BoFeN1—questioning the existence of enzymatic Fe(II) oxidation. *Geobiology* 11:396. <https://doi.org/10.1111/gbi.12040>.
  41. Wu WF, Swanner ED, Hao LK, Zeitvogel F, Obst M, Pan YX, Kappler A. 2014. Characterization of the physiology and cell-mineral interactions of the marine anoxygenic phototrophic Fe(II) oxidizer *Rhodovulum iodolum*—implications for Precambrian Fe(II) oxidation. *FEMS Microbiol Ecol* 88:503–515. <https://doi.org/10.1111/1574-6941.12315>.
  42. Hao L, Guo Y, Byrne JM, Zeitvogel F, Schmid G, Ingino P, Li J, Neu TR, Swanner ED, Kappler A, Obst M. 2016. Binding of heavy metal ions in aggregates of microbial cells, EPS and biogenic iron minerals measured in-situ using metal- and glycoconjugates-specific fluorophores. *Geochim Cosmochim Acta* 180:66–96. <https://doi.org/10.1016/j.gca.2016.02.016>.
  43. Hegler F, Posth NR, Jiang J, Kappler A. 2008. Physiology of phototrophic iron(II)-oxidizing bacteria: implications for modern and ancient environments. *FEMS Microbiol Ecol* 66:250–260. <https://doi.org/10.1111/j.1574-6941.2008.00592.x>.
  44. Ng DHP, Kumar A, Cao B. 2016. Microorganisms meet solid minerals: interactions and biotechnological applications. *Appl Microbiol Biotechnol* 100:6935–6946. <https://doi.org/10.1007/s00253-016-7678-2>.
  45. Miot J, Benzerara K, Morin G, Kappler A, Bernard S, Obst M, Ferard C, Skouri-Panet F, Guigner JM, Posth N, Galvez M, Brown GE, Guyot F. 2009. Iron biomineralization by anaerobic neutrophilic iron-oxidizing bacteria. *Geochim Cosmochim Acta* 73:696–711. <https://doi.org/10.1016/j.gca.2008.10.033>.
  46. Li BH, Pan X, Zhang DY, Lee DJ, Al-Misned FA, Mortuza MG. 2015. Anaerobic nitrate reduction with oxidation of Fe(II) by *Citrobacter freundii* strain PXL1—a potential candidate for simultaneous removal of As and nitrate from groundwater. *Ecol Eng* 77:196–201. <https://doi.org/10.1016/j.ecoleng.2015.01.027>.
  47. Vallance P, Charles I. 1998. Nitric oxide as an antimicrobial agent: does NO always mean NO? *Gut* 42:313–314. <https://doi.org/10.1136/gut.42.3.313>.
  48. Chan CS, Fakra SC, Emerson D, Fleming EJ, Edwards KJ. 2011. Lithotrophic iron-oxidizing bacteria produce organic stalks to control mineral growth: implications for biosignature formation. *ISME J* 5:717–727. <https://doi.org/10.1038/ismej.2010.173>.
  49. Gauger T, Byrne JM, Konhauser KO, Obst M, Crowe S, Kappler A. 2016. Influence of organics and silica on Fe(II) oxidation rates and cell-mineral aggregate formation by the green-sulfur Fe(II)-oxidizing bacterium *Chlorobium ferrooxidans* KoFox—implications for Fe(II) oxidation in ancient oceans. *Earth Planet Sci Lett* 443:81–89. <https://doi.org/10.1016/j.epsl.2016.03.022>.
  50. Straub KL, Rainey FA, Widdel F. 1999. *Rhodovulum iodolum* sp. nov., and *Rhodovulum robiginosum* sp. nov., two new marine phototrophic ferrous-iron-oxidizing purple bacteria. *Int J Syst Bacteriol* 49:729–735. <https://doi.org/10.1099/00207713-49-2-729>.
  51. Kappler A, Newman DK. 2004. Formation of Fe(III)-minerals by Fe(II)-oxidizing photoautotrophic bacteria. *Geochim Cosmochim Acta* 68:1217–1226. <https://doi.org/10.1016/j.gca.2003.09.006>.
  52. Pantke C, Obst M, Benzerara K, Morin G, Ona-Nguema G, Dippon U, Kappler A. 2012. Green rust formation during Fe(II) oxidation by the nitrate-reducing *Acidovorax* sp. strain BoFeN1. *Environ Sci Technol* 46:1439–1446. <https://doi.org/10.1021/es2016457>.
  53. Miot J, Benzerara K, Morin G, Bernard S, Beysac O, Larquet E, Kappler A, Guyot F. 2009. Transformation of vivianite by anaerobic nitrate-reducing iron-oxidizing bacteria. *Geobiology* 7:373–384. <https://doi.org/10.1111/j.1472-4669.2009.00203.x>.
  54. Kampschreur MJ, Kleerebezem R, de Vet WWJM, van Loosdrecht MCM. 2011. Reduced iron induced nitric oxide and nitrous oxide emission. *Water Res* 45:5945–5952. <https://doi.org/10.1016/j.watres.2011.08.056>.
  55. Konhauser KO. 1998. Diversity of bacterial iron mineralization. *Earth Sci Rev* 43:91–121. [https://doi.org/10.1016/S0012-8252\(97\)00036-6](https://doi.org/10.1016/S0012-8252(97)00036-6).
  56. Preston LJ, Shuster J, Fernández-Remolar D, Banerjee NR, Osinski GR, Southam G. 2011. The preservation and degradation of filamentous bacteria and biomolecules within iron oxide deposits at Rio Tinto, Spain. *Geobiology* 9:233–249. <https://doi.org/10.1111/j.1472-4669.2011.00275.x>.
  57. Najem T, Langley S, Fortin D. 2016. A comparison of Fe(III) reduction rates between fresh and aged biogenic iron oxides (BIOS) by *Shewanella*

- putrefaciens CN32. *Chem Geol* 439:1–12. <https://doi.org/10.1016/j.chemgeo.2016.06.006>.
58. Kelso BHL, Smith RV, Laughlin RJ, Lennox SD. 1997. Dissimilatory nitrate reduction in anaerobic sediments leading to river nitrite accumulation. *Appl Environ Microbiol* 63:4679–4685.
59. Wang M, Hu R, Zhao J, Kuzyakov Y, Liu S. 2016. Iron oxidation affects nitrous oxide emissions via donating electrons to denitrification in paddy soils. *Geoderma* 271:173–180. <https://doi.org/10.1016/j.geoderma.2016.02.022>.
60. Hamilton JL, Lowe RH. 1981. Organic-matter and N-effects on soil nitrite accumulation and resultant nitrite toxicity to tobacco transplants. *Agron J* 73:787–790. <https://doi.org/10.2134/agronj1981.000219620073000500010x>.
61. Van Cleemput O, Samater AH. 1995. Nitrite in soils: accumulation and role in the formation of gaseous N compounds. *Fert Res* 45:81–89. <https://doi.org/10.1007/BF00749884>.
62. Ehrenreich A, Widdel F. 1994. Anaerobic oxidation of ferrous iron by purple bacteria, a new-type of phototrophic metabolism. *Appl Environ Microbiol* 60:4517–4526.
63. Emmerich M, Bhansali A, Losekann-Behrens T, Schroder C, Kappler A, Behrens S. 2012. Abundance, distribution, and activity of Fe(II)-oxidizing and Fe(III)-reducing microorganisms in hypersaline sediments of Lake Kasin, southern Russia. *Appl Environ Microbiol* 78:4386–4399. <https://doi.org/10.1128/AEM.07637-11>.
64. Stookey LL. 1970. Ferrozine—a new spectrophotometric reagent for iron. *Anal Chem* 42:779–781. <https://doi.org/10.1021/ac60289a016>.
65. Hazrin-Chong NH, Manefield M. 2012. An alternative SEM drying method using hexamethyldisilazane (HMDS) for microbial cell attachment studies on sub-bituminous coal. *J Microbiol Methods* 90:96–99. <https://doi.org/10.1016/j.mimet.2012.04.014>.
66. Bray DF, Bagu J, Koegler P. 1993. Comparison of hexamethyldisilazane (HMDS), Peldri II, and critical-point drying methods for scanning electron microscopy of biological specimens. *Microsc Res Tech* 26:489–495. <https://doi.org/10.1002/jemt.1070260603>.